



Contents lists available at ScienceDirect



# Applied Catalysis A: General

journal homepage: [www.elsevier.com/locate/apcata](http://www.elsevier.com/locate/apcata)

## Gold as active phase of BN-supported catalysts for lactose oxidation

Nathalie Meyer, Coralie Renders, Raphaël Lanckman, Michel Devillers, Sophie Hermans\*

Université catholique de Louvain, Institut de la Matière Condensée et des Nanosciences (IMCN), Place Louis Pasteur 1/3, B-1348 Louvain-la-Neuve, Belgium

### ARTICLE INFO

#### Article history:

Received 15 September 2014

Received in revised form

29 December 2014

Accepted 5 January 2015

Available online xxx

#### Keywords:

Gold

Boron nitride

Lactose

Regeneration

Selectivity

### ABSTRACT

Au/h-BN catalysts have been prepared by wet impregnation in order to combine the high activity of gold with the promising h-BN support to optimize the catalytic performances in lactose oxidation. After 1 h reaction, the catalysts were more active than all the Pd/h-BN catalysts described in previous works: 100% yield was reached after 2 h for a Au/h-BN catalyst prepared in water and containing only 1 wt.% of gold. The influence of  $\alpha$ -Al<sub>2</sub>O<sub>3</sub>,  $\gamma$ -Al<sub>2</sub>O<sub>3</sub> and C<sub>black</sub> as supports for Au was compared to h-BN and Au/ $\alpha$ -Al<sub>2</sub>O<sub>3</sub>. C<sub>black</sub> was the most active. All of them exhibited 100% selectivity toward lactobionic acid. After a second run, Au/ $\gamma$ -Al<sub>2</sub>O<sub>3</sub> presented a loss of selectivity and all were less active than during their first run. Au/h-BN and Au/ $\alpha$ -Al<sub>2</sub>O<sub>3</sub> have been regenerated and a thermal treatment permits to keep the catalysts active with 100% selectivity. Au/h-BN was the most active after regeneration thanks to the more facile poison removal from its surface and the high stability of boron nitride.

© 2015 Elsevier B.V. All rights reserved.

### 1. Introduction

Carbohydrates represent an important source of renewable raw materials because of their large availability, high framework complexity and independency from fossil energies. In this work, we focus on lactose, which is an important by-product of the dairy industry, and whose production is estimated at about 1.2 million tons per year [1]. Because of its low solubility and sweetness, as well as certain intolerance of many people in the world, it presents a limited usage. However, with this surplus and low cost, there is an interest in the research of innovative processes for transforming lactose for applications in the food and pharmaceutical industries [2–4]. The valuable products that can be obtained from it are lactulose, lactitol, lactobionic acid, lactosucrose, and galactooligosaccharides [2]. A recently published review focuses on the main characteristics, uses and physiological effects of lactobionic acid (LBA) which has high potential applications as a bioactive molecule [5]. The main commercial utilization of LBA derives from its antioxidant, chelating and emulsifying properties [5–11]. It is an antioxidant compound which can replace formalin as an organ preservation liquid with the advantage of being less toxic [8,12].

In the literature, the heterogeneous catalysts reported to carry out lactose oxidation are mainly based on noble metals (Au, Pd, Bi-Pd, Pt) supported on Al<sub>2</sub>O<sub>3</sub>, SiO<sub>2</sub>, TiO<sub>2</sub>, CeO<sub>2</sub>, carbon or zeolites [13–21]. Few studies have reported that supporting Au

nano-particles on alumina, titania or ceria allowed obtaining moderate to high conversions and selectivities [13,14,18,22]. Many studies have been carried out with Au supported catalysts in general and they have all demonstrated the promising future of this metal in heterogeneous catalysis [23–34] which was related to quantum size effects within very small gold particles [34–37]. Moreover, gold presents in general a high resistance to deactivation, especially by oxygen poisoning, which makes it a more stable active phase than other noble metals such as palladium or platinum. For example, Mirescu and Prusse studied the influence of several parameters on the activity of Au/Al<sub>2</sub>O<sub>3</sub> and Au/TiO<sub>2</sub> catalysts for lactose oxidation [13]. They have shown that at 80 °C, the activity of the catalysts was much lower than at 40 °C because of the lower solubility of oxygen and that Au/Al<sub>2</sub>O<sub>3</sub> were deactivated in acidic medium as well as at strong alkaline pH. The recycling was also studied with Au/Al<sub>2</sub>O<sub>3</sub> and a loss of activity was observed but the catalysts were still able to carry out the reaction with 99% of selectivity in LBA. In a recent study, Au/mesoporous silica catalysts have been used and exhibited excellent performances by reaching 100% selectivity and 100% conversion after 100 min in lactose oxidation [2,3]. In our previous works, hexagonal boron nitride (h-BN) has been evaluated as catalyst support and it was shown that it is an appropriate candidate to obtain high selectivity in the oxidation of lactose [38]. The best Pd/h-BN catalysts presented a particle size distribution comprised between 3 and 15 nm with no particles smaller than 3 nm [39]. In the present work, we will try to combine the high catalytic activity of gold with the promising support which is boron nitride, in order to obtain catalysts presenting optimized activities and selectivities in the oxidation of lactose to

\* Corresponding author. Tel.: +32 10 472810; fax: +32 10 472330.

E-mail address: [sophie.hermans@uclouvain.be](mailto:sophie.hermans@uclouvain.be) (S. Hermans).

lactobionic acid. In addition to the evaluation of Au/h-BN catalysts, we will compare boron nitride with three other supports, namely  $\alpha$ -Al<sub>2</sub>O<sub>3</sub>,  $\gamma$ -Al<sub>2</sub>O<sub>3</sub> and C<sub>black</sub>. The recycling of Au-based catalysts will be also investigated and the regeneration of some catalysts by two methods will be described.

## 2. Experimental

### 2.1. Materials

The selected supports were a commercial alumina ( $\gamma$ -Al<sub>2</sub>O<sub>3</sub>, Sigma-Aldrich,  $S_{BET} \approx 173 \text{ m}^2 \text{ g}^{-1}$ ), a commercial hexagonal boron nitride (h-BN, Sigma-Aldrich,  $S_{BET} \approx 23 \text{ m}^2 \text{ g}^{-1}$ ) and a commercial carbon black (C<sub>black</sub>, Timcal,  $S_{BET} \approx 63 \text{ m}^2 \text{ g}^{-1}$ ). A batch of the alumina support was calcined in air at 1000 °C for 24 h to give  $\alpha$ -Al<sub>2</sub>O<sub>3</sub> ( $S_{BET} \approx 16 \text{ m}^2 \text{ g}^{-1}$ ). The gold precursor was gold (III) chloride trihydrate (HAuCl<sub>4</sub>·3H<sub>2</sub>O, Sigma-Aldrich, 99.9%) in all cases.

### 2.2. Wet impregnation synthesis (WI)

In a typical experiment, 2.5 g of support was suspended in 50 mL of solvent and stirred for 15 min. The gold precursor, HAuCl<sub>4</sub>·3H<sub>2</sub>O, was dissolved in 25 mL of the same solvent and added dropwise within 30 min to the support suspension. Then, the suspension was stirred for a further 15 min. The catalyst was chemically reduced at 80 °C by addition of 6 mL formalin (formaldehyde 37 wt.% aqueous solution, Sigma-Aldrich) or NaBH<sub>4</sub> previously dissolved in the same solvent (0.1 g/mL). Finally, the catalyst was separated by filtration, washed with the corresponding solvent and dried overnight. The filtrates containing potentially non-adsorbed Au were analyzed by atomic absorption spectrometry. The solvents used in this preparation method were deionized water, acetonitrile (Riedel-de-Haën, 99.5%) or a mixture 50:50 v/v water/methanol (VWR, 99.9%).

The reproducibility of the synthesis method was checked by preparing two catalysts (Au.WI-2) in the same manner and these were shown to present the same characteristics in terms of metallic percentages at the support surface as well as Au/B ratio determined by XPS.

### 2.3. Regeneration of the catalysts

#### 2.3.1. Chemical regeneration

The used catalyst was dispersed in 50 mL of water and the suspension was stirred for 15 min. A solution of NaBH<sub>4</sub> 0.1 g/mL was added and the suspension was stirred for 1 h. The catalyst was then filtered, washed and dried overnight.

#### 2.3.2. Thermal regeneration

The used catalyst was calcinated in air flow (500 cm<sup>3</sup>/h) at 500 °C for 10 h. The catalyst was then reduced in a tubular oven for 2 h at 200 °C under H<sub>2</sub>(5%)/Ar(95%) flow.

### 2.4. Oxidation of lactose

All catalytic tests were performed in a thermostatized double-walled glass reactor. The pH of the lactose solution was measured continuously by a combined AgCl/Ag Beckman electrode calibrated with buffer solutions of pH 7 and 10 (Fluka). An automatic titration device Metrohm 842 Titrand was used to neutralize the acids formed over time with KOH (Riedel-de-Haën, ≥85%). Constant stirring was ensured by a mechanical stirrer (Heidolph RZR 2051 electronic). Oxygen was introduced into the solution at a constant flow rate. The detailed experimental conditions used for lactose oxidation are given in Supplementary information (S1). Aliquots were taken each hour in order to follow the reaction by HPLC. The experiments were stopped after 1 or 4 h. The catalyst was recovered

by filtration and the filtrate was analyzed by HPLC. Because selectivity was 100% in all cases, the lactose conversion always equals the yield in lactobionic acid.

### 2.5. Physico-chemical characterization techniques

The catalysts were characterized by X-ray photoelectron spectroscopy (XPS), transmission electron microscopy (TEM), X-ray powder diffraction (XRD) and CO chemisorption.

X-ray photoelectron spectroscopy (XPS) was performed on a SSI-X-probe (SSX-100/206) spectrometer from Fisons. The samples were pressed on little stainless steel cell-cups and then placed on an insulating home-made ceramic carousel with a nickel grid positioned 3 mm above the sample surface, to avoid differential charging effects: a floodgun set at 8 eV was used for charge stabilization. The C<sub>1s</sub> binding energy of carbon (C—C, H) set at 284.8 eV was used as internal standard value. Data treatment was performed with the CasaXPS program (Casa software Ltd.). The analytical peaks used were C<sub>1s</sub>, Au<sub>4f</sub>, Na<sub>1s</sub>, Cl<sub>2p</sub>, O<sub>1s</sub>, N<sub>1s</sub>, Al<sub>2p</sub> and B<sub>1s</sub>. The following constraints were used for photopeak decomposition in the case of Au: intensity ratios: I(Au 4f<sub>7/2</sub>)/I(Au 4f<sub>5/2</sub>) = 1.33, FWHM ratio = 1,  $\Delta(\text{Au } 4\text{f}_{5/2} - \text{Au } 4\text{f}_{7/2}) = 3.67 \text{ eV}$ .

TEM images were obtained with a LEO 922 omega energy filter transmission electron microscope operating at 200 kV. The samples were suspended in hexane under ultrasonic treatment, and then allowed to settle to discard the biggest particles. A drop of the supernatant was deposited on a holey carbon film supported on a copper grid, which was dried overnight under vacuum at room temperature, before introduction in the microscope. Histograms of particles size distribution were determined by measuring 100 particles for each catalyst.

XRD analyses were performed with a D5000 Siemens diffractometer equipped with a copper source ( $\lambda_{K\alpha} = 154.18 \text{ pm}$ ). The samples were supported on quartz monocrystals. The crystalline phases detected were identified by reference to the JCPDS-ICDD database. The Pd particles sizes were extracted from X-ray diffraction measurements by using the Debye-Scherrer equation [40]:

$$B = \frac{k\lambda}{s \cos \theta}$$

where  $k$  is a constant taken as 1.00 here,  $\lambda$  is the wavelength of X-ray radiation (CuK $\alpha$  = 0.1541 nm),  $s$  is the crystalline size,  $\theta$  is the diffraction angle,  $B$  is the line width at half maximum height.

The quantification of Au in the synthesis filtrates and the catalytic reaction mixtures was performed by atomic absorption analysis, using a Perkin-Elmer 3110 spectrometer equipped with an air-acetylene flame atomizer. The calibration curve (from 1 to 15 mg/L Au) was realized with standard solutions obtained by dilution of a commercial gold (1 g/mL, Acros) solution.

HPLC analysis was performed on a Waters system equipped with a refractive index 2414 detector and a UV 2998 photodiode array detector. To quantify the lactobionic acid, an Aminex BioRad HPX-87C column was used, with CaSO<sub>4</sub> 1.2 mmol/L as eluent, a flow of 0.8 mL/min, a column temperature of 80 °C and 10  $\mu\text{L}$  of injected volume. To quantify the remaining lactose and the potential lactulose formed (lactose's isomer), a Carbohydrate Transgenic CarboSep CHO682 column was used, with mQH<sub>2</sub>O (18 MΩ at 25 °C) as eluent, a flow of 0.4 mL/min, a column temperature of 80 °C and 10  $\mu\text{L}$  of injected volume.

### 2.6. Calculation of the specific activity

In order to make comparisons with the literature [13] the specific activity was calculated for several catalysts, as follows: Specific activity =  $\frac{\text{substrate}}{\text{time} \times \text{metal}}$  (mmol min<sup>-1</sup> g<sup>-1</sup>) where

**Table 1**

Au/h-BN catalysts prepared by wet impregnation.

Code	Impregnation solvent	Au (wt.%) engaged	Au <sup>c</sup> (wt.%) (AAS)	Particle size (XRD) <sup>d</sup>	Au at.% (XPS)	Au/B × 100 (XPS)
Au.WI-1 <sup>a</sup>	H <sub>2</sub> O	4.92	4.9	25	0.14	0.28
Au.WI-2 <sup>a</sup>	H <sub>2</sub> O	1.02	1.0	34	0.06	0.15
Au.WI-3 <sup>a</sup>	CH <sub>3</sub> CN	5.07	5.0	18	0.52	1.1
Au.WI-4 <sup>a</sup>	CH <sub>3</sub> CN	3.08	3.1	17	0.38	0.84
Au.WI-5 <sup>a</sup>	CH <sub>3</sub> CN	1.00	1.0	12	0.10	0.21
Au.WI-6 <sup>b</sup>	CH <sub>3</sub> OH-H <sub>2</sub> O	4.95	3.0	47	0.017	0.04
Au.WI-7 <sup>b</sup>	CH <sub>3</sub> OH-H <sub>2</sub> O	0.99	0.99	38	0.0090	0.02

<sup>a</sup> Reducing agent = NaBH<sub>4</sub>.<sup>b</sup> Reducing agent = formaldehyde.<sup>c</sup> Au loading determined by difference after atomic absorption analysis of the synthesis filtrates.<sup>d</sup> Average particle size determined by XRD using Scherrer equation.

substrate = amount of converted substrate at 10% conversion, time = time when 10% conversion was reached (in min), metal = amount of the active metal in the catalyst.

### 3. Results and discussion

Four supports were selected in the present study (h-BN,  $\alpha$ -Al<sub>2</sub>O<sub>3</sub>,  $\gamma$ -Al<sub>2</sub>O<sub>3</sub> and C<sub>black</sub>) and their textural properties are presented in Supplementary information (S2). The nitrogen isotherms are shown in Fig. S3. h-BN and  $\alpha$ -Al<sub>2</sub>O<sub>3</sub> can be considered as non-porous, with intergranular macropores, while C<sub>black</sub> presents some micropores. This latter was chosen because it has a surface area close to h-BN. Only  $\gamma$ -Al<sub>2</sub>O<sub>3</sub> develops some surface area due to the presence of pores. The major difference between the supports is the amount of oxygenated groups on their surfaces, following the decreasing order:  $\gamma$ -Al<sub>2</sub>O<sub>3</sub> > C<sub>black</sub> >  $\alpha$ -Al<sub>2</sub>O<sub>3</sub> > h-BN.

Blank tests have been carried out with the supports alone and no lactose conversion was observed. The h-BN and  $\alpha$ -Al<sub>2</sub>O<sub>3</sub> supports alone before and after tests have been analyzed by XPS (see Table S4). No major change was observed.

#### 3.1. Au/h-BN catalysts prepared by wet impregnation (WI)

The catalysts prepared by WI together with the synthesis solvents used as well as the metal loading determined by atomic absorption spectrometry are summarized in Table 1. When water or acetonitrile were used as impregnation solvents, all the metal was deposited on the h-BN support. For the catalyst prepared in water-methanol (Au.WI-6) with 5 wt.% of Au, it can be observed that the amount of gold not deposited on the support is non-negligible.

Table 1 presents also the average metallic particle size determined by XRD using the Scherrer equation and the amount of gold present at the catalyst surface as analyzed by XPS. No surface poisoning by chloride was detected by XPS. The lowest average particle sizes have been observed for the samples prepared in acetonitrile while the highest are present when using water-methanol. The smallest particles are obtained when the most hydrophobic solvent is used. Indeed, the hydrophobicity increases following acetonitrile > water-methanol > water [41,42]. Au.WI-6 and Au.WI-7 present a very small Au at.% at the boron nitride surface, in relation with their low loadings.

All the gold XPS peaks are well aligned and correspond to the gold metallic phase (S5). A difference in intensity is nevertheless observed. This could be because a softer reducer would take more time to produce Au<sup>0</sup>, favoring growth of the gold particles, while NaBH<sub>4</sub> will nucleate more rapidly the particles at the support surface giving smaller particles for a same amount of metal engaged.

Fig. 1 presents respectively TEM images of Au.WI-2 and Au.WI-7. The catalyst prepared in water-methanol mixture exhibits some huge aggregates with a size of 200 nm (Fig. 1(b)) while the metallic particles in Au.WI-2 are of the order of 10 nm (Fig. 1(a)). XRD

**Table 2**

Time to convert lactose entirely with Au/h-BN catalysts.

Code	Au loading (wt.%)	X <sub>Lactose</sub> (%) after 4 h	Time for complete conversion
Au.WI-1	4.9	100	2h36
Au.WI-2	1.0	100	2h
Au.WI-3	5.0	100	1h28
Au.WI-4	3.1	100	1h23
Au.WI-5	1.0	100	2h43
Au.WI-6	3.0	0	n.d.
Au.WI-7	0.99	0	n.d.

analyses do not give the same particle sizes than TEM but this is due to the fact that an average size is obtained by XRD and moreover the smallest particles are not detected by XRD because they are amorphous. These images permit to explain the weak percentage of gold detected for Au.WI-6 and Au.WI-7 by XPS, which analyzes only 5–10 nm thickness.

All these catalysts have been tested in the oxidation of lactose into lactobionic acid (LBA) for 4 h. At this time, except for the two catalysts prepared in water/methanol, they all reach 100% yield with 100% selectivity. However, the time to convert fully lactose differs from one catalyst to the other (Table 2). The curves showing the evolution of lactose conversion over time are presented in Supplementary information (S6). Au.WI-2 contains only 1% of Au and converts lactose as fast as Au.WI-1 loaded with 5% of metal. These results show the high activity of Au/h-BN catalysts, much higher than the best Pd/h-BN reported previously [38,39] and prepared using the same method. We can point out that Au(1 wt.%)/h-BN catalysts are, after 1 h, even more active than their homologues Pd(1 and 5 wt.%)/h-BN after 4 h [39]. As expected, the catalysts prepared in water/methanol mixture were not able to carry out the transformation.

At the end of the catalytic tests, the filtrates were analyzed by atomic absorption spectroscopy and we observed weak Au losses for the catalysts prepared in acetonitrile only (4.08%, 7.21% and 6.19% of the total Au amount engaged for Au.WI-3, Au.WI-4 and Au.WI-5, respectively). For this reason, the next steps will be investigated with the catalysts prepared in water only.

#### 3.2. Diffusional limitations

Before studying several parameters that could influence the catalytic results with Au/h-BN materials, the absence of diffusional limitation had to be checked given their very high activities. Boron nitride is a “non-porous”/macroporous support and should not exhibit internal diffusion limitations referring to the reactant diffusion throughout the porous network. In order to verify this, the catalyst can be ground and the catalytic activity should not change. Moreover, when the reactants flow is too low, the observed rate could also be controlled by external diffusion and therefore not represent the actual rate of the catalyzed reaction [42–44]. This

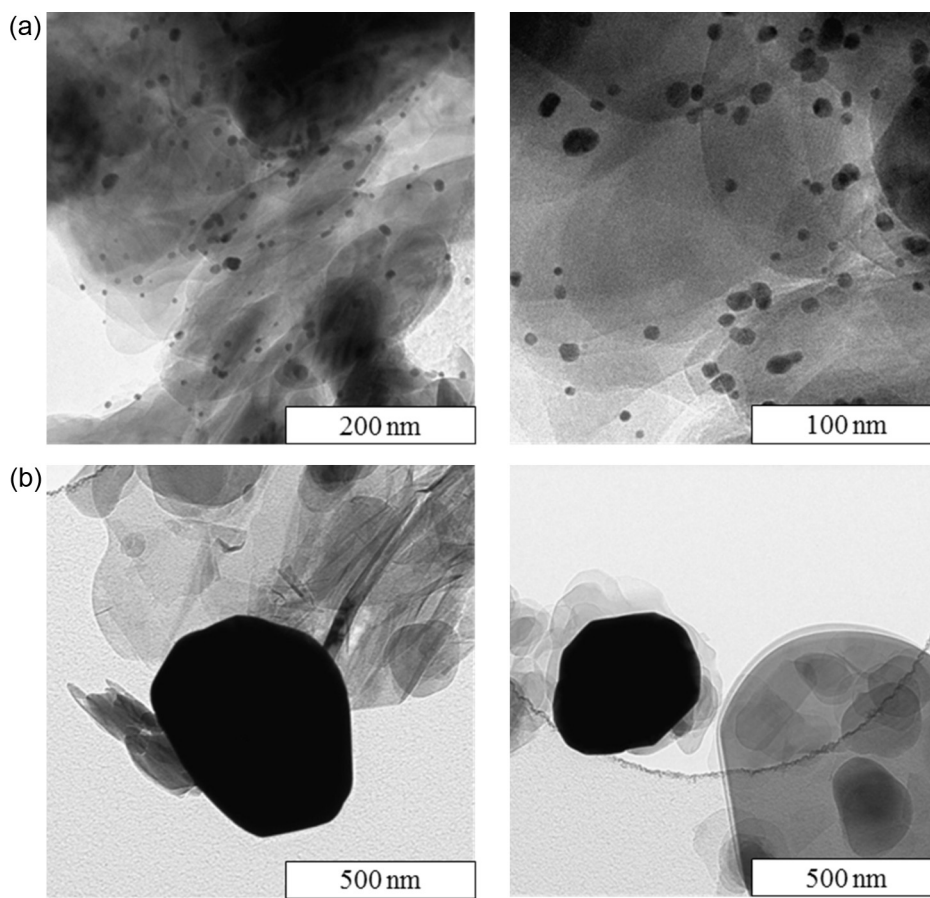


**Fig. 1.** TEM images of (a) Au\_WI-2 prepared in water (Au 1 wt.%/h-BN) and (b) Au\_WI-7 prepared in water-methanol (Au 1 wt.%/h-BN).

phenomenon can be detected by increasing the stirring rate. The last potential problem is the total occupancy of the active sites by reactants and the rate limiting factor is, in this case, the surface reactivity. By decreasing the catalyst amount, the number of active sites decreases as well leading in principle, to a lower reaction rate in the same proportions. The control experiments for diffusional limitations have been carried out with the Au\_WI-2 catalyst synthesized in water and containing 1 wt.% Au. Six catalytic tests were followed over time by taking out samples of the reaction mixture every 30 min, for 4 h and analyzing them by HPLC (S7).

Lactobionic acid selectivity was 100% in each case. The yields in lactobionic acid at 1000 or 1500 rpm stirring rate were similar whatever the amount of catalyst engaged. Grinding had no effect on the catalytic performances and when the amount of catalyst was halved, the lactobionic acid yield decreased proportionally. All these observations confirm that there is no diffusional limitation.

### 3.3. Influence of the support nature

It has been described in the literature that the support can have an important effect on the activity. For example, Murzin et al. studied lactose oxidation with several supports, mainly  $\text{Fe}_3\text{O}_4$  and  $\text{Al}_2\text{O}_3$  and they showed that Au(2 wt.%)/ $\text{Al}_2\text{O}_3$  was the most active with a LBA selectivity of 95% at 20% lactose conversion. Au/ $\text{Fe}_3\text{O}_4$  catalyst was shown to be more prone to deactivation because of oxygen coverage on the surface [18]. Au/h-BN supported catalysts are very active in the selective oxidation of lactose, therefore  $\alpha\text{-Al}_2\text{O}_3$ ,  $\gamma\text{-Al}_2\text{O}_3$  and  $\text{C}_{\text{black}}$  have been selected for comparison with boron nitride given their similar textural properties in the case of  $\alpha\text{-Al}_2\text{O}_3$  and  $\text{C}_{\text{black}}$ , and the presence of more surface hydroxyls in the case of

**Table 3**  
Gold catalysts prepared by WI on different supports.

Code	Support	Au loading <sup>a</sup> (wt.%)	Time at 100% conversion <sup>b</sup> (min)	$Y_{\text{LBA}}$ after 1 h reaction <sup>c</sup> (%)
Au_WI-2	h-BN	1.0	120	68
Au_WI-8	$\alpha\text{-Al}_2\text{O}_3$	1.0	93	87
Au_WI-9	$\gamma\text{-Al}_2\text{O}_3$	1.0	106	81
Au_WI-10	$\text{C}_{\text{black}}$	1.0	162	53

<sup>a</sup> Au loading determined by difference after atomic absorption analysis of the synthesis filtrates.

<sup>b</sup> Determined by automatic titration.

<sup>c</sup> Determined by HPLC.

$\gamma\text{-Al}_2\text{O}_3$ . **Table 3** presents catalysts prepared on the four supports synthesized by the same wet impregnation method.

The curves presenting the evolution of activity for 4 h are shown in SI (S9).  $\alpha\text{-Al}_2\text{O}_3$  permits to obtain the most rapidly total conversion of lactose.  $\gamma\text{-Al}_2\text{O}_3$  allows also a high conversion of lactose followed by h-BN while  $\text{C}_{\text{black}}$  gives lower results. In order to make comparisons, the yield after 1 h reaction was determined by HPLC (**Table 3**). The same trend was observed. In all cases, 100% selectivity was obtained whatever lactose conversion reached, therefore  $Y_{\text{LBA}}$  equals the conversion. The catalytic filtrates have been analyzed by atomic absorption spectroscopy and no Au losses were observed during the oxidation reaction. The four catalysts were characterized by TEM and XPS before and after 1 h reaction. **Table 4** shows the XPS surface atomic percentage and Au/B,C or Al atomic ratios. The first observation is that the higher the surface atomic Au percentage, the higher the catalytic activity. Except for  $\gamma\text{-Al}_2\text{O}_3$  where an obvious decrease can be observed, the XPS results do not vary much after a catalytic test. TEM images of Au\_WI-2

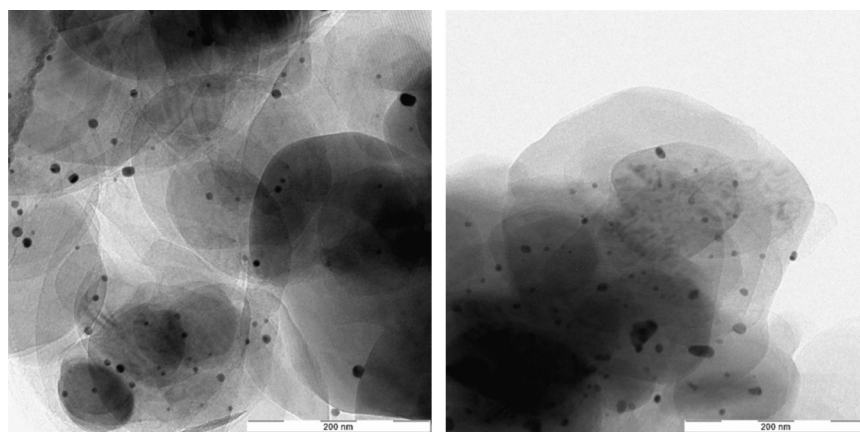


**Fig. 2.** TEM images of Au.WI-2 after a catalytic test.

**Table 4**

XPS results of Au(1 wt.%) catalysts supported on different supports before use, after one and two uses ( $t = 1$  h).

Code	Support	Au at.% (XPS)			Au/(B,C,Al) × 100 (XPS)		
		BT <sup>a</sup>	1st use	2nd use	BT <sup>a</sup>	1st use	2nd use
Au.WI-2	h-BN	0.064	0.067	0.063	0.15	0.15	0.14
Au.WI-8	$\alpha$ -Al <sub>2</sub> O <sub>3</sub>	0.65	0.67	0.90	2.0	2.4	3.0
Au.WI-9	$\gamma$ -Al <sub>2</sub> O <sub>3</sub>	0.25	0.079	0.20	0.74	0.29	0.72
Au.WI-10	C <sub>black</sub>	0.041	0.040	0.031	0.042	0.04	0.033

<sup>a</sup> Before test.

(Au/h-BN) show a relatively homogeneous distribution of the particles on the support as described previously (Fig. 1(a)), before but also after the catalytic test (Fig. 2). The particle size distribution was also established by measuring around 100 particles (S10). The histograms before and after catalytic test are similar, confirming the XPS results. The average size of gold particles is comprised between 5 and 15 nm, with only very few particles below 3 nm. Fig. 3 shows TEM images of Au.WI-8, prepared on alpha alumina, before and after a catalytic test. It comes out here that the particle size distribution is more heterogeneous than in the case of hexagonal boron nitride as confirmed by the histograms presented in S11. Moreover, after the catalyst use, small particles seem to be formed,

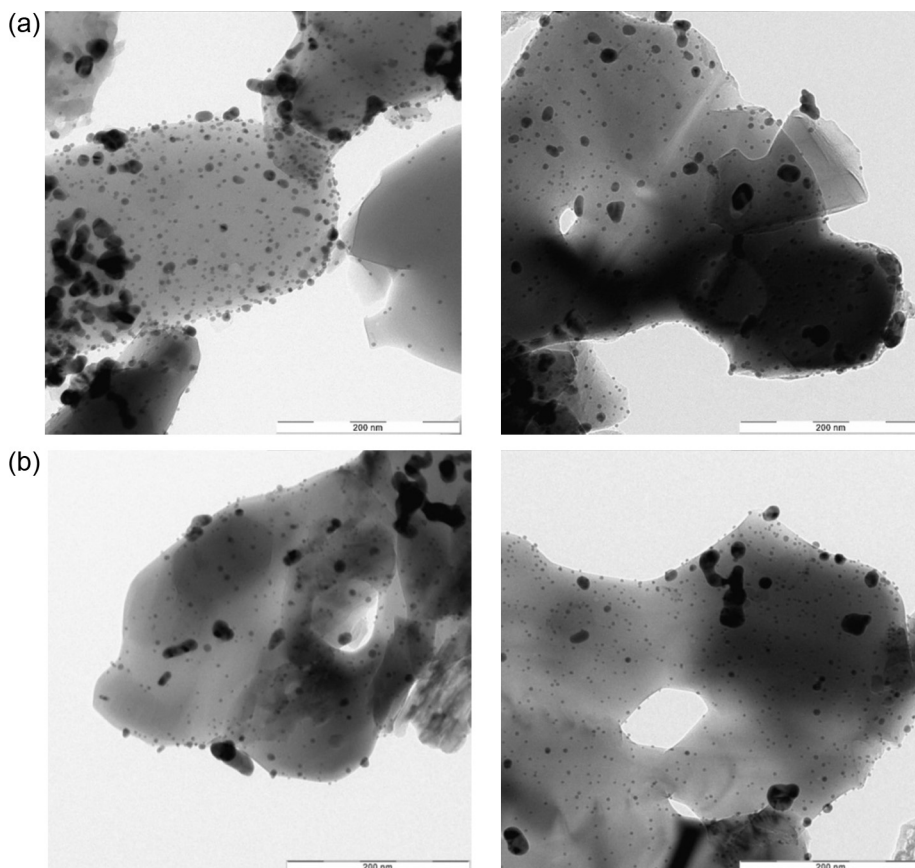


**Fig. 3.** TEM images of Au.WI-8, (a) before a catalytic test and (b) after a catalytic test.

leading to an increase in the proportion of particles with a size comprised between 3 and 5 nm. At some places, bigger agglomerates are present while smaller particles can be found at other locations. TEM images have also been taken for the catalysts prepared on  $\gamma\text{-Al}_2\text{O}_3$  and  $\text{C}_{\text{black}}$ . However, for these two samples, due to the lack of contrast between support and metal particles in the TEM images, the size distribution could not be determined precisely. In the case of  $\gamma\text{-Al}_2\text{O}_3$ , a mix of small particles and bigger aggregates are present before and after being tested in the oxidation reaction (S12). S13 shows images of Au\_WI-10 (Au/ $\text{C}_{\text{black}}$ ), before test but the gold particles are not easily visualized. The curves presenting the evolution of the activity with time (S9) permit to determine the specific activity of the catalysts. For Au\_WI-8 supported on  $\alpha\text{-Al}_2\text{O}_3$ , the specific activity is  $12 \text{ mmol min}^{-1} \text{ g}^{-1}$ . The catalyst supported on boron nitride presents a specific activity of  $7.5 \text{ mmol min}^{-1} \text{ g}^{-1}$  which is higher than the best Pd/h-BN catalyst described in a previous work [38] that displayed an activity of  $2.5 \text{ mmol min}^{-1} \text{ g}^{-1}$ . The gold catalysts presented here are competitive with the best gold catalysts for lactose oxidation found in the literature. Indeed, Mirescu and Prusse obtained a specific activity of  $18 \text{ mmol min}^{-1} \text{ g}^{-1}$  for a Au/TiO<sub>2</sub> catalyst [13].

### 3.4. Recycling of the catalysts

In the literature, studies about catalyst recyclability in sugars oxidation are quite scarce. Even though Au supported catalysts have been shown to be the best for lactose oxidation, they are very often deactivated at prolonged reaction times and uses [45,46]. In this section, the recycling of the catalysts prepared by wet impregnation on boron nitride and on the three other supports will be studied.

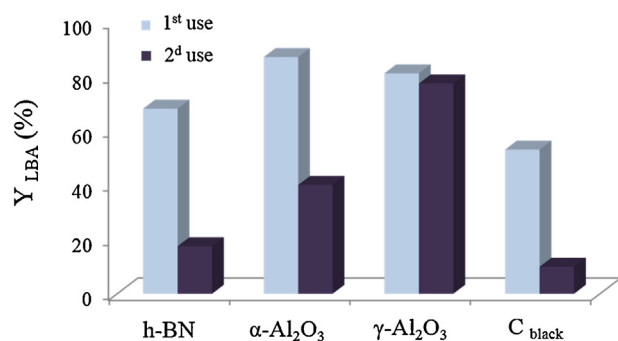


**Fig. 4.** 1st and 2nd use of Au(1 wt.%) catalysts supported on several supports in lactose oxidation after 1 h reaction.

The catalysts will be characterized by TEM and XPS in order to see the impact of several uses.

#### 3.4.1. Recycling of 1 wt.% Au catalysts prepared on different supports

A loss of 48% of yield for Au/h-BN catalyst after a second use is observed while 45% of loss for Au/ $\alpha\text{-Al}_2\text{O}_3$  and 50% for Au/ $\text{C}_{\text{black}}$  appeared. After a second use, the catalyst supported on  $\gamma\text{-Al}_2\text{O}_3$  gives the best yield in LBA with only 3% of loss (Fig. 4). However, this catalyst suffers from a loss in selectivity because of the formation of 2-keto-lactobionic acid. This might be attributable to the presence of hydroxyl functions at the support surface as shown in a previous work [39], where the selectivity was shown to be influenced negatively when the number of surface oxygenated groups increased. Indeed, the XPS Au/Al ratio decreases after one test suggesting a particle agglomeration. Thus, during the second run, the

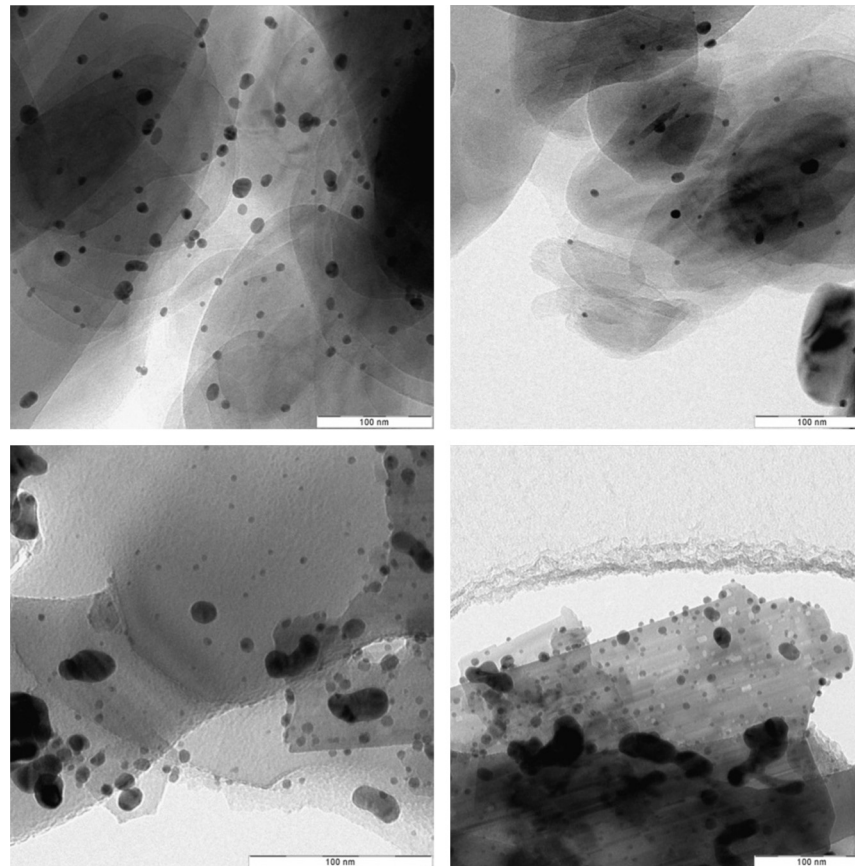


**Fig. 5.** TEM images of Au\_WI-2 (Au/h-BN): above and Au\_WI-8 (Au/ $\alpha\text{-Al}_2\text{O}_3$ ) after two uses in lactose oxidation: below.

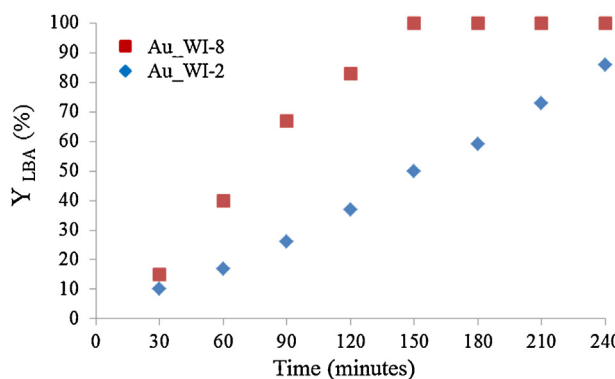


**Fig. 6.** Monitoring of the oxidation of lactose into lactobionic acid for 4 h with Au\_WI-8 (Au/α-Al<sub>2</sub>O<sub>3</sub>) and Au\_WI-2 (Au/h-BN) during their 2nd run.

—OH groups present at the surface become more accessible and are able to influence the selectivity. We can conclude that the —OH functions are deleterious for the selectivity but beneficial for the stability. α-Al<sub>2</sub>O<sub>3</sub> gives better results than h-BN and C black after a second use with still 100% selectivity. No Au losses were observed after two catalytic tests. XPS characterization data of the catalysts before use, after one test and after a second test are presented in **Table 4**. The catalyst prepared on h-BN does not show any change in Au at.% or in Au/B atomic ratios over the uses. When C<sub>black</sub> is used, the surface Au% decreases after the second use which might correspond to an agglomeration of the particles. On the opposite, with α-Al<sub>2</sub>O<sub>3</sub> as support, an increase is observed which could be due to a re-distribution of the metallic particles.

TEM images after two catalytic tests (**Fig. 5**) have been taken and the particle size distributions before, after one and two runs were determined for the catalysts prepared on h-BN and α-Al<sub>2</sub>O<sub>3</sub>. For Au/h-BN catalyst (Au\_WI-2), the particle size distribution profile remains unchanged while for Au/α-Al<sub>2</sub>O<sub>3</sub>, some large particles are present after two runs in addition to smaller ones. After the second run, the proportion of particles inferior to 3 nm decreases significantly in favor of particles with a size superior to 10 nm.

#### 3.4.2. Identification of deactivation causes of Au/h-BN and Au/α-Al<sub>2</sub>O<sub>3</sub> catalysts

A monitoring over time was realized during the second run of these two catalysts for 4 h (**Fig. 6**). Both catalysts give relatively high activities after 4 h, with an optimal selectivity toward lactobionic acid. However, compared to their first run, a non-negligible loss of activity was observed. Here, the possible causes of deactivation that can be considered are leaching, sintering or poisoning. We will discuss them in turn in the following sections.

**3.4.2.1. Leaching.** The cause of deactivation of these two catalysts is not leaching because no Au has been found in the catalytic test filtrates.

**3.4.2.2. Sintering.** In order to verify if the activity loss during the second run is due to sintering, the characterization data of the catalysts after one run have to be analyzed. For Au/h-BN, no particle growth was observed by TEM and the particle size distribution profile remains unchanged after one test indicating that no sintering occurred. The majority of particles have a size comprised between 5 and 10 nm. The proportion of particles smaller than 3 nm remains inferior to 10% which is favorable in lactose oxidation as described in a previous work [39]. In addition, Au/B ratios and Au at.% determined by XPS do not vary after one test. Concerning Au/α-Al<sub>2</sub>O<sub>3</sub>, the metallic particles are not growing either. However, they tend to decrease after one test giving a higher proportion of particles smaller than 3 nm, as observed in particle size distribution

**Table 5**  
XPS characterization results for Au\_WI-2 and Au\_WI-8.

Code	% O	% C	O/B	C/B
h-BN	3.0	3.9	0.063	0.082
h-BN blank <sup>a</sup>	3.6	3.8	0.075	0.080
Au_WI-2	4.7	4.8	0.11	0.11
Au_WI-2 1st run	5.4	2.7	0.12	0.058
Au_WI-2 2nd run	4.1	4.5	0.091	0.10
	% O	% C	O/Al	C/Al
α-Al <sub>2</sub> O <sub>3</sub>	51	14	1.5	0.41
α-Al <sub>2</sub> O <sub>3</sub> blank <sup>a</sup>	54	12	1.6	0.34
Au_WI-8	55	12.	1.7	0.38
Au_WI-8 1st run	55	16	2.0	0.57
Au_WI-8 2nd run	56	13	1.9	0.42

<sup>a</sup> Supports alone tested in oxidation reaction.

histograms. XPS Au/Al ratios confirm this observation because it increases after one run corresponding to higher metallic dispersion. The fact that during the second run this catalyst is not as active is explained by the presence of these particles smaller than 3 nm which play a detrimental role in this reaction.

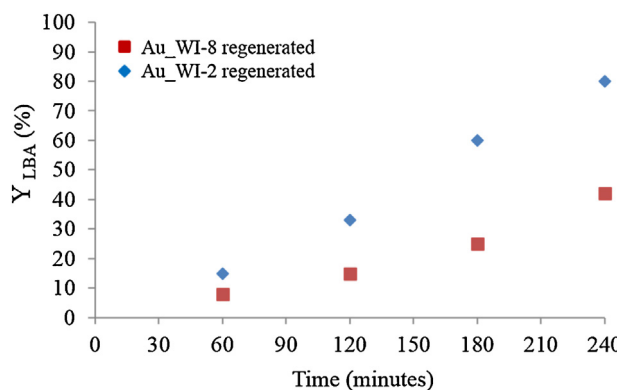
**3.4.2.3. Poisoning.** Poisoning of the metal surface by strongly adsorbed species such as impurities, products, by-products or oxygen can occur [47]. In order to determine if a surface anchoring of sugars appears on the supports without metallic phase, two catalytic tests with the supports alone have been carried out and these were analyzed before and after tests by XPS. The atomic percentages of C and O on the surface of h-BN or α-Al<sub>2</sub>O<sub>3</sub> before and after test were similar (**Table 5**). The possible poisons are molecular oxygen, lactose or lactobionic acid. Molecular oxygen can poison the active phase which might then be oxidized. The oxidation state of gold does not vary over the catalyst runs for Au\_WI-2 (S14) but seems to be slightly different for Au\_WI-8 after two runs (S15). However, Au is usually less sensitive to O<sub>2</sub> poisoning than other metals so this cause can be excluded here.

Carbon and oxygen surface percentages as well as O/(B or Al) and C/(B or Al) have been determined by XPS and compared before, after one and after a second run for the Au catalysts. In both cases, the oxygen % as well as O/B or O/Al ratios increase after the first run (**Table 5** and S16). The XPS O<sub>1s</sub> peaks are similar before and after test for both catalysts and correspond probably to adsorbed oxygen. In the case of Au/α-Al<sub>2</sub>O<sub>3</sub> (Au\_WI-8), C at.% increases after one test, which may indicate sugar or product poisoning (S16). When the sugar or LBA is adsorbed on Au particles, hydrogen-bridge bonds can appear between the OH functions of the support and —O— atom of lactose or the C=O of LBA. It was already shown in the literature that LBA can have an inhibiting effect on lactose conversion by catalyst deactivation [21]. Hence we can conclude that poisoning is probably the cause of activity losses.

#### 3.5. Regeneration of the catalysts

The recycling tests presented in the previous section have shown that the efficiency of our catalysts decreases significantly along the successive runs. In order to counteract the loss of efficiency of our catalysts, two methods of regeneration have been tested for Au/α-Al<sub>2</sub>O<sub>3</sub> and Au/h-BN. These methods aim at either cleaning up the poisoned catalyst surface, re-disperse the active phase or to reduce gold to the metallic oxidation state. The first used method is chemical while the second one is thermal.

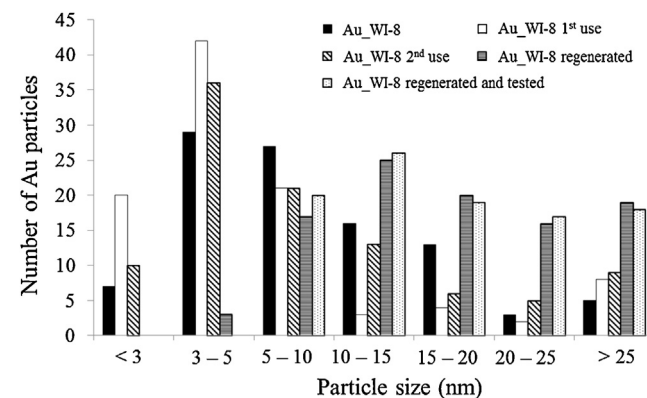
Considering that the metallic state is the active phase for the oxidation of lactose, NaBH<sub>4</sub> as a reducer was used to “re-activate” this phase if a thin layer of oxide had formed during the reaction. Indeed, for Au\_WI-8, a slight shift in Au binding energy was observed after



**Fig. 7.** Monitoring of lactose oxidation into lactobionic acid for 4 h with Au\_WI-8 (Au/α-Al<sub>2</sub>O<sub>3</sub>) and Au\_WI-2 (Au/h-BN) thermally regenerated.

two runs (by XPS) which could correspond to Au<sup>+1</sup> species. The activity after chemical regeneration was followed during 4 h and it came out that the chemical regeneration has a negative impact on the catalytic performances because about 30% lactose conversion after 4 h was obtained (S17) while before this regeneration, almost 100% was obtained after 4 h as shown previously in Fig. 6.

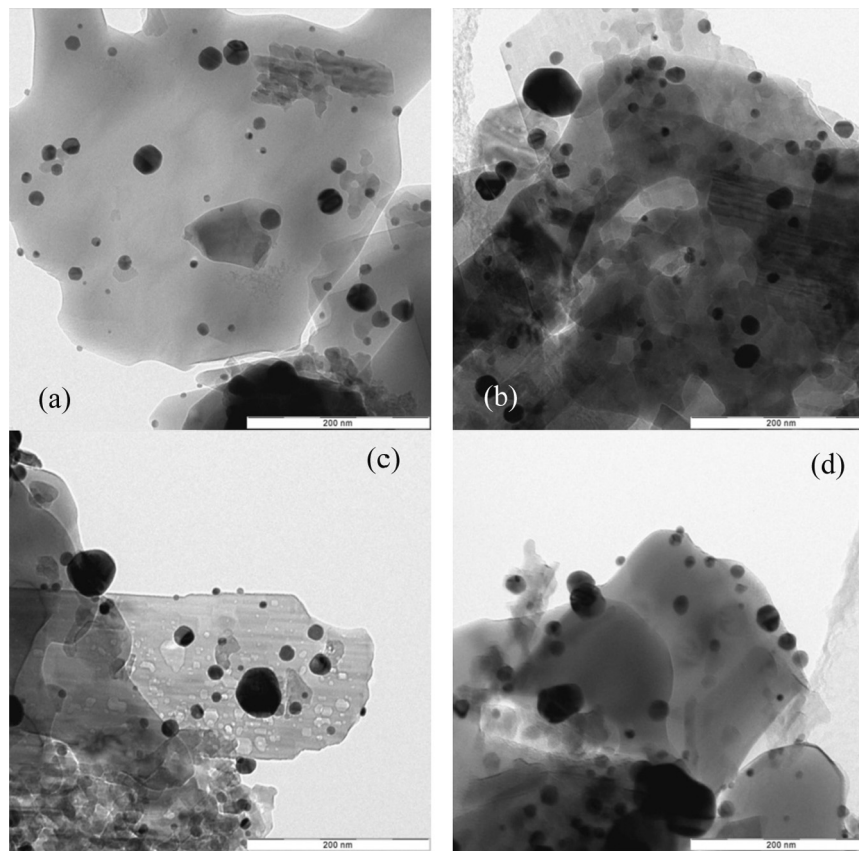
The thermal regeneration of the catalysts has also been carried out for the catalysts supported on α-Al<sub>2</sub>O<sub>3</sub> and h-BN only. Indeed, at high temperature, γ-Al<sub>2</sub>O<sub>3</sub> begins to be transformed in α-Al<sub>2</sub>O<sub>3</sub> and C<sub>black</sub> is burnt. Au/h-BN and Au/α-Al<sub>2</sub>O<sub>3</sub> after two runs have been calcined at 500 °C and reduced at 200 °C for 2 h with H<sub>2</sub>(5%)/Ar(95%). These catalysts were monitored for 4 h in lactose oxidation (Fig. 7). The selectivity in LBA was 100% for both catalysts. The treatment applied failed to restore the initial catalyst effectiveness. However, the regenerated Au/h-BN showed a



**Fig. 9.** Particle size distribution in Au/α-Al<sub>2</sub>O<sub>3</sub> catalyst before test, after one run and after two runs, after regeneration and tested after regeneration.

better activity than Au/α-Al<sub>2</sub>O<sub>3</sub>. It should be noted that the calcination temperature could be optimized because above 200 °C gold is spontaneously reduced, and 500 °C might not be enough to burn organic poisons.

These catalysts have been characterized by XPS after the regeneration and after use of the regenerated catalysts for both chemical and thermal treatments. The atomic Au% and the Au/B or Au/Al ratios obtained for the two catalysts are presented in Table 6. Concerning the chemical regeneration, it gives lower Au at.% and lower Au/B or Al ratios after treatment for both catalysts leading to a lower dispersion of the metallic phase. The use of these regenerated catalysts causes a re-dispersion of the metallic particles given the increased Au% at the catalyst surface and the higher Au/B, Al obtained after test. Concerning the catalysts thermally regenerated, the catalyst prepared on α-Al<sub>2</sub>O<sub>3</sub> displayed a decrease

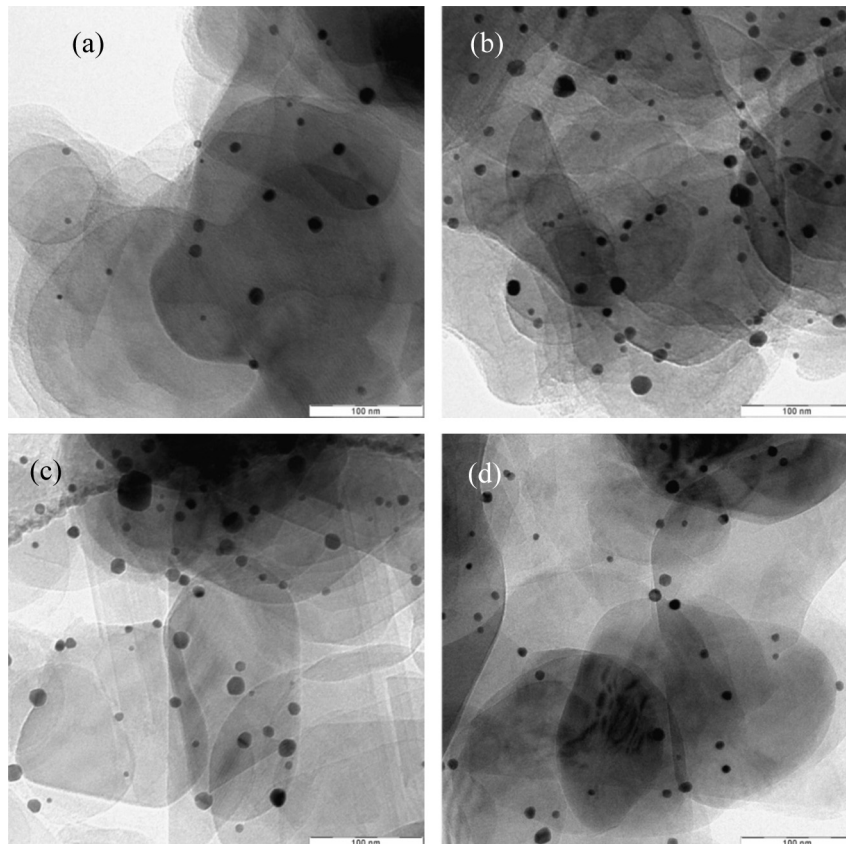
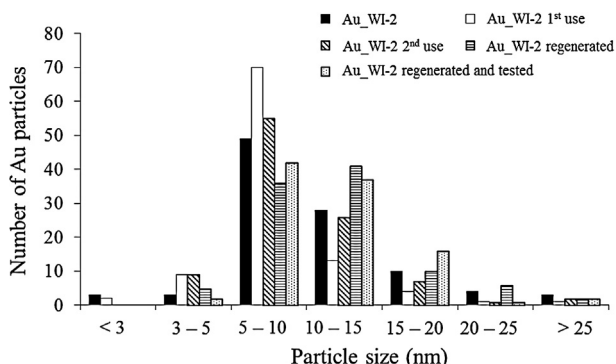


**Fig. 8.** TEM images of Au\_WI-8: (a) and (b) after thermal regeneration and (c) and (d) Au\_WI-8 after test of regenerated catalyst.

**Table 6**

XPS results of Au\_WI-2 and Au\_WI-8 after two runs, regeneration and tested regenerated catalysts.

Code	After two runs		Chemically regenerated		Tested after chemical regeneration	
	Au at.%	Au/(B,Al) × 100	Au at.%	Au/(B,Al) × 100	Au at.%	Au/(B,Al) × 100
Au_WI-8 $\alpha$ -Al <sub>2</sub> O <sub>3</sub>	0.90	3.0	0.33	1.1	0.53	1.9
Au_WI-2 h-BN	0.063	0.14	0.035	0.098	0.066	0.14
Thermally regenerated						
Au_WI-8 $\alpha$ -Al <sub>2</sub> O <sub>3</sub>	0.90	3.0	0.37	1.3	0.31	1.12
Au_WI-2 h-BN	0.063	0.14	0.075	0.28	0.041	0.090

**Fig. 10.** TEM images of Au\_WI-2: (a) and (b) after thermal regeneration and (c) and (d) after test of regenerated catalyst.**Fig. 11.** Particle size distribution in Au/h-BN catalysts before test, after one run and after two runs, after regeneration and tested after regeneration.

in the atomic Au% and of Au/Al ratio after regeneration, probably due to particles agglomeration. In the case of boron nitride supported catalyst, an increase was observed pointing toward re-dispersion. Au XPS spectra of both catalysts, after thermal regeneration and use, show the presence of metallic gold (S18). The fact

that Au/h-BN is more active after thermal regeneration than Au/ $\alpha$ -Al<sub>2</sub>O<sub>3</sub> could be due to removal of the poisons of the active sites. During the regeneration process, the surface of gold is cleaned more easily in the case of BN thanks to the absence of functional groups on the support. But XPS analyses of carbon at.% and C/B or C/Al atomic ratios did not permit to prove this hypothesis. TEM images of the thermally regenerated and tested catalysts (Fig. 8) show, in the case of Au\_WI-8 supported on  $\alpha$ -Al<sub>2</sub>O<sub>3</sub> that the main difference before and after regeneration is the proportion of particles smaller than 3 nm which are absent for this latter. Particle size distributions of the catalysts after regeneration and after test allow confirming this observation (Fig. 9). Indeed, no particle inferior to 3 nm is present anymore for the regenerated catalyst or after its use in lactose oxidation while many much larger particles appear. The thermal regeneration implies an increase in gold particle size with  $\alpha$ -Al<sub>2</sub>O<sub>3</sub> as support. Concerning the catalyst prepared on boron nitride, the thermal regeneration seems to be more beneficial on the particle distribution which is more homogeneous after regeneration as shown on the TEM images (Fig. 10). The particle size distributions for Au\_WI-2 after regeneration and for the tested regenerated catalyst have been measured and as in the case of Au/ $\alpha$ -Al<sub>2</sub>O<sub>3</sub>, the proportion of particles smaller than 3 nm decreased significantly

(Fig. 11). However, the amount of very large particles ( $>20\text{ nm}$ ) did not increase as much. This shows that BN is beneficial for the regeneration step.

#### 4. Conclusion

Gold is known for its surprisingly high activity in heterogeneous catalysis, the objective of the present work was to combine the high activity of gold with the promising h-BN support in order to optimize the catalytic performances in lactose oxidation. Au/h-BN catalysts have been prepared by the wet impregnation method. Some tests have shown that we were not in diffusional regime. After 1 h reaction, the prepared Au/h-BN catalysts were more active than all the Pd/h-BN materials described previously and were even competitive with the best Au catalysts on different supports reported in the literature. The influence of  $\alpha\text{-Al}_2\text{O}_3$ ,  $\gamma\text{-Al}_2\text{O}_3$  and  $\text{C}_{\text{black}}$  as supports for Au has been compared to h-BN. It was shown that the catalyst prepared on  $\alpha\text{-Al}_2\text{O}_3$  is the most active and competitive. During their first run, they have all demonstrated 100% selectivity toward LBA. The recycling was also studied with the Au catalysts. After a 2nd run, a non-negligible loss of activity was observed except for  $\gamma\text{-Al}_2\text{O}_3$ . However, the selectivity for this catalyst was not 100% anymore. The causes of deactivation were studied for Au/ $\alpha\text{-Al}_2\text{O}_3$  and Au/h-BN catalysts. The XPS characterization analyses have shown that a poisoning of the metallic phase takes place during the catalytic reaction because the at.% of O as well as O/B or O/Al ratios increased after one run. The poisoning is more consequent for Au/ $\alpha\text{-Al}_2\text{O}_3$  regarding the atomic C% that increased also after one run. A regeneration step was carried out for Au/ $\alpha\text{-Al}_2\text{O}_3$  and Au/h-BN in order to recover the effectiveness of the fresh catalysts. Thermal regeneration permits to keep the catalysts active with 100% selectivity. After thermal regeneration, the catalyst supported on boron nitride presented the highest activity and the most homogeneous particle size distribution. This could be explained by the presence of oxygenated functions on  $\alpha\text{-Al}_2\text{O}_3$  which stabilize surface poisons and might hinder cleaning during regeneration.

#### Acknowledgements

The authors wish to thank the Fonds de la Recherche Scientifique (FRS-FNRS) with the assistance of the Fédération Wallonie-Bruxelles and the Belgian National Lottery, as well as the Université catholique de Louvain for funding. This work was also partially funded by the Belgian State (Belgian Science Policy, IAP Project INANOMAT N° P6/17). We are grateful as well to Jean-François Stassys, Pierre Eloy and Pascale Lipnik for technical assistance and useful discussions.

#### Appendix A. Supplementary data

Supplementary data associated with this article can be found, in the online version, at <http://dx.doi.org/10.1016/j.apcata.2015.01.009>.

#### References

- [1] J. Kowalczyk, U. Prusse, H. Berndt, I. Pitsch, (2007). Method for selective carbohydrate oxidation using supported gold catalysts, US Patent 20070112186A1.
- [2] J.G. Zadow, *J. Dairy Sci.* 67 (1984) 2654–2679.
- [3] L.-F. Gutierrez, S. Hamoudi, K. Belkacemi, *Appl. Catal. A: Gen.* 402 (2011) 94–103.
- [4] L.-F. Gutierrez, S. Hamoudi, K. Belkacemi, *Int. Dairy J.* 26 (2012) 103–111.
- [5] K.J. Foster, S. Lin, C. Turk, *Crit. Care Nurs. Clin. N. Am.* 22 (2010) 341–350.
- [6] Y. Paik, K. Lee, H. Han, *Yonsei Med. J.* 46 (2005) 399–407.
- [7] B. Sharma, P. Sharma, A. Agrawal, S. Sarin, *Gastroenterology* 137 (2009) 885–891.
- [8] K. Hicks, F. Parrish, *Carbohydr. Res.* 82 (1980) 393–397.
- [9] M. Kozampel, M. Kurantz, J. Craig, K. Hicks, *Biotechnol. Prog.* 11 (1995) 592–595.
- [10] M. Adamczak, D. Charubin, W. Bednarski, *Chem. Pap.* 6 (2009) 111–116.
- [11] L. Mayer, B. Kranz, L. Fisher, *J. Biotechnol.* 145 (2010) 389–393.
- [12] J.H. Southard, F.O. Belzer, *Annu. Rev. Med.* 46 (1995) 235–247.
- [13] A. Mirescu, U. Prusse, *Appl. Catal. B: Environ.* 70 (2007) 644–652.
- [14] J. Kuusisto, A.V. Tokarev, E.V. Murzina, M.U. Roslund, J.-P. Mikkola, D.Y. Murzin, T. Salmi, *Catal. Today* 121 (2007) 92–99.
- [15] A. Abbadi, K.F. Gotlieb, J.B.M. Meiberg, H. van Bekkum, *Appl. Catal. A: Gen.* 156 (1997) 105–115.
- [16] S. Karski, I. Witonka, J. Goluchowska, *J. Mol. Catal. A: Chem.* 245 (2006) 225–230.
- [17] A.V. Tokarev, D.Y. Murzin, *Microporous Mesoporous Mater.* 113 (2008) 122–131.
- [18] E.V. Murzina, A.V. Tokarev, K. Kordas, H. Karhu, J.-P. Mikkola, D.Y. Murzin, *Catal. Today* 131 (2008) 385–392.
- [19] L. Prati, M. Rossi, *J. Catal.* 176 (1998) 552–560.
- [20] K.B. Kokoh, N. Alonso-Vante, *J. Appl. Electrochem.* 36 (2006) 147–151.
- [21] D.Y. Murzin, E.V. Murzina, A.V. Tokarev, J.-P. Mikkola, *Russ. J. Electrochem.* 45 (2009) 1017–1026.
- [22] A.V. Tokarev, E.V. Murzina, J.P. Mikkola, J. Kuusisto, L.M. Kustov, D.Y. Murzin, *Chem. Eng. J.* 134 (2007) 153–161.
- [23] A. Montilla, M. Castillo, M. Sanz, A. Olano, *Food Chem.* 90 (2005) 883–890.
- [24] G.C. Bond, *Molecules* 17 (2012) 1716–1743.
- [25] G.C. Bond, *Gold Bull.* 5 (1972) 11–13.
- [26] G.J. Hutchings, *J. Catal.* 96 (1985) 292–295.
- [27] C.H. Christensen, B. Jorgensen, J. Rass-Hansen, K. Egeblad, R. Madsen, S.K. Klitgaard, S.M. Hansen, M.R. Hansen, H.C. Andersen, A. Rijsager, *Angew. Chem. Int. Ed.* 45 (2006) 4648–4651.
- [28] A.S.L. Hashmi, *Chem. Rev.* 107 (2007) 3180–3211.
- [29] A. Corma, M.E. Domíne, *Chem. Commun.* (2005) 4042–4044.
- [30] N. Lopez, T.V.J. Janssens, B.S. Clausen, Y. Xu, M. Mavrikakis, T. Bligaard, J.K. Norskov, *J. Catal.* 223 (2004) 232–235.
- [31] C. Baatz, N. Decker, U. Prüss, *J. Catal.* 258 (2008) 165–169.
- [32] L. Prati, G. Martra, *Gold Bull.* 32 (1999) 96–101.
- [33] M.S. Chen, D.W. Goodman, *Catal. Today* 111 (2006) 22–32.
- [34] S. Schimpf, M. Lucas, C. Mohr, U. Rodemerck, A. Brückner, J. Radnik, H. Hofmeister, P. Claus, *Catal. Today* 72 (2002) 63–78.
- [35] M. Haruta, *Catal. Today* 36 (1997) 153–166.
- [36] G.C. Hutchings, *Catal. Today* 100 (2005) 55–61.
- [37] M. Haruta, *Nature* 437 (2005) 1098–1099.
- [38] N. Meyer, K. Bekaert, D. Pirson, M. Devillers, S. Hermans, *Catal. Commun.* 29 (2012) 170–174.
- [39] N. Meyer, D. Pirson, M. Devillers, S. Hermans, *Appl. Catal. A: Gen.* 467 (2013) 463–473.
- [40] N. von Weymarn, M. Hujanen, M. Leisola, *Process Biochem.* 37 (2002) 1207–1213.
- [41] A.I. Vogel, A.R. Tatchell, B.S. Furnis, A.J. Hannaford, P.W.G. Smith, *Vogel's Textbook of Practical Organic Chemistry*, 5th ed., Pearson Education India, 1989.
- [42] S.J. Suresh, V. Naik, *J. Chem. Phys.* 116 (2002) 4212–4220.
- [43] U.K. Singh, M.A. Vannice, *Appl. Catal. A: Gen.* 213 (2001) 1–24.
- [44] T.K. Sherwood, *Pure Appl. Chem.* 10 (1965) 595–610.
- [45] S.W. Weller, *Catal. Rev. Sci. Eng.* 34 (1992) 227–280.
- [46] B.T. Kusema, D.Y. Murzin, *Catal. Sci. Technol.* 3 (2013) 297–307.
- [47] M. Besson, P. Gallezot, *Catal. Today* 57 (2000) 127–141.